

DOI: 10.1002/cmdc.201200587

Novel Schiff-Base-Derived FabH Inhibitors with Dioxygenated Rings as Antibiotic Agents

Yang Zhou,^[a] Qian-Ru Du,^[a] Jian Sun,^[a] Jing-Ran Li,^[a] Fei Fang,^[a] Dong-Dong Li,^[a]
Yong Qian,^[a] Hai-Bin Gong,^{*[b]} Jing Zhao,^[a] and Hai-Liang Zhu^{*[a]}

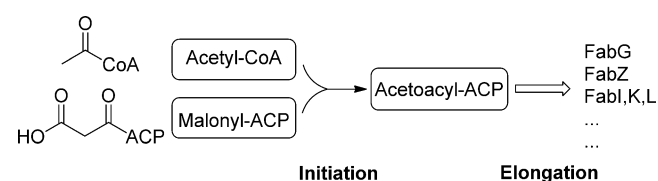
Fatty acid biosynthesis plays a vital role in bacterial survival and several key enzymes involved in this biosynthetic pathway have been identified as attractive targets for the development of new antibacterial agents. Of these promising targets, β -ketoacyl-acyl carrier protein (ACP) synthase III (FabH) is the most attractive target that could trigger the initiation of fatty acid biosynthesis and is highly conserved among Gram-positive and -negative bacteria. Designing small molecules with FabH inhibitory activity displays great significance for developing antibiotic agents, which should be highly selective, nontoxic and broad-spectrum. In this manuscript, a series of novel Schiff

base compounds were designed and synthesized, and their biological activities were evaluated as potential inhibitors. Among these 21 new compounds, (*E*)-*N*-((3,4-dihydro-2*H*-benzo[*b*][1,4]dioxepin-7-yl)methylene)hexadecan-1-amine (**10**) showed the most potent antibacterial activity with a MIC value of 3.89–7.81 μM^{-1} against the tested bacterial strains and exhibited the most potent *E. coli* FabH inhibitory activity with an IC_{50} value of 1.6 μM . Docking simulation was performed to position compound **10** into the *E. coli* FabH active site to determine the probable binding conformation.

Introduction

Fatty acid synthesis (FAS) is an essential metabolic process for the viability and growth of cells in prokaryotic organisms. Controlling this pathway in some key enzymes or proteins is a valuable route for developing new antibacterial agents. Bacteria generate fatty acids (components of phospholipids) through type II fatty acid synthesis (FAS II), which generally includes two stages: initiation and elongation (Scheme 1). This is in contrast to mammalian type I fatty acid synthase (FAS I), which is a multi-enzyme complex process, with each of the reactions performed by a separate enzyme. Thus, targeting one or two dominant catalytic units in the FAS II pathway represents a rea-

sonable tactic in the development of new antibiotics. For example, the two natural products, cerulenin and thiolactomycin (Figure 1), are inhibitors of the condensing enzymes both FabB and FabF, and both compounds show antibacterial activity.^[1] In addition, the bacterial FAS system and proteins bear little ho-



Scheme 1. FabH-catalyzed initiation reaction of fatty acid biosynthesis. Abbreviations: acyl carrier protein (ACP).

[a] Dr. Y. Zhou,[†] Dr. Q.-R. Du,[†] Dr. J. Sun, Dr. J.-R. Li, Dr. F. Fang, Dr. D.-D. Li, Dr. Y. Qian, Prof. J. Zhao, Prof. H.-L. Zhu
State Key Laboratory of Pharmaceutical Biotechnology, Nanjing University
Hankou Road, Nanjing 210093 (P.R. China)
E-mail: zhuhl@nju.edu.cn

[b] Dr. H.-B. Gong
Xuzhou Central Hospital, Xuzhou 221009 (P.R. China)

[[†]] These authors contributed equally to this work.

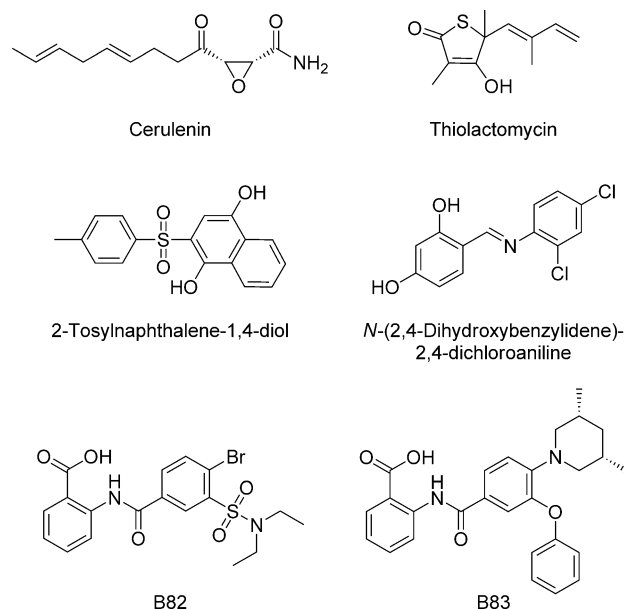


Figure 1. Several reported antibacterial agents targeting the fatty acid synthesis (FAS) pathway: cerulenin,^[1] thiolactomycin,^[1] 2-tosyl-naphthalene-1,4-diol (2008),^[6] benzylidene derivatives (e.g., **6a**),^[7] diethyl sulfonamide derivatives (e.g., B82),^[5] and [3-phenoxybenzoylamino]benzoic acid derivatives (e.g., B83).^[5]

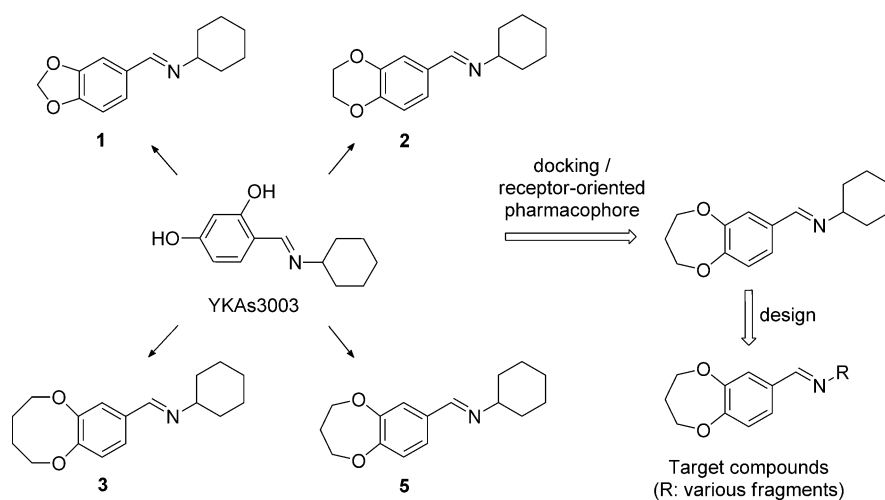
mology to the human system, indicating that type II-selective inhibitors could be identified with high probability.^[1]

Among these enzymes, β -ketoacyl-acyl carrier protein (ACP) synthase III (FabH) plays an essential role in the biosynthesis of bacterial fatty acids, as it initiates the FAS cycle by catalyzing the first condensation step between acetyl-CoA and malonyl-ACP (Scheme 1). Moreover, FabH proteins from both Gram-positive and -negative bacteria are highly conserved at the sequence and structural level. When considering bacteria resistant to known therapies, FabH should become a more attractive target for the development of new antibacterial agents than other important FAS enzymes. Several optimized FabH inhibitors presented in Figure 1 have been optimized for the enzyme-inhibitor complex,^[2,3] and accordingly, their structure-activity relationships (SARs) have been described over many years.^[4-7] We start our research based on these related studies.

Recently, Brinster et al.^[8] reported that, when the culture medium is supplemented with fatty acids or human serum, FAS II is not essential in *Streptococcus agalactiae* (*Lactobacillales*). This not only challenged the general knowledge on targeting FAS II in Gram-positive pathogens but also triggered an explosive debate on whether these observations with *S. agalactiae* could be reasonably generalized for all Gram-positive or, further, Gram-negative bacteria. So far, the views of this issue are essentially divided into two opposite opinions, and a majority tends to the conservative side, which is supported by the finding by Balemans et al.^[9] that fatty acids were unable to rescue *Staphylococcus aureus* when treated with an enoyl-ACP reductase (FabI) inhibitor. Moreover, Joshua et al.^[10] point out that important details on how Gram-positive bacteria uptake and use the exogenous fatty acids are still unclear, and these could not explain various reports on the efficacy of inhibitors of fatty acid synthesis against *S. aureus* in mouse models.^[11-13] Interestingly, they did not construct an *S. aureus* FabH knockout model that was a fatty acid auxotroph, and this might leave an unknown role for FabH in the *S. aureus* strain when using exogenous fatty acids. Therefore, much work towards drug development in the pathway of bacterial fatty acid synthesis remains. Our study is based on the presumption that disturbing the FAS cycle would influence cell viability and growth in prokaryotic organisms.

Molecular docking and structure-based pharmacophore in silico screening are two effective methods to identify novel and specific ligands or fragments. Because the in silico screening process can systematically analyze all possible binding modes between a compound and protein in the active site, it is an applied methodology of rational drug design.^[14-16] Iden-

tification of protein active sites and analysis of receptor-ligand interactions are the two important steps for generating pharmacophore maps. These are mainly composed of sets of interactions (chemical features or functionalities), aligned in three-dimensional space, and include several features along with excluded volume regions derived from receptor atom positions.^[17,18] In this manuscript, we firstly attempt to design four novel Schiff bases (1-3, 5) derived from YKAs3003^[19] that maintain the structure of the cyclohexylamine moiety. The design strategy and experimental flowchart are shown in Scheme 2:



Scheme 2. Design strategy: a lead compound (YKAs3003) initiates a series of novel antibiotic agents.

the molecular docking of the five compounds (including YKAs3003) was performed using the CDOCKER protocol,^[20] and receptor-oriented pharmacophore model based on *Escherichia coli* FabH protein complex (PDB: 1HNJ) could be generated by using the Discovery Studio software.^[20] The combined analysis of the docking study and pharmacophore screening shows that compound 5 with the heptane ring is most suitable as a lead compound for an optimized scaffold for the design of new FabH inhibitors. The designed inhibitors on the basis of compound 5 were synthesized and evaluated against two Gram-negative bacterial strains, *E. coli* and *Pseudomonas fluorescens*, and two Gram-positive bacterial strains, *Bacillus subtilis* and *S. aureus*. In addition, several potent antibacterial agents were subsequently assessed for the corresponding FabH inhibitory activity in vitro.

Results and Discussion

Molecular docking and development of a FabH pharmacophore model

The synthesis of the four kinds of benzaldehyde analogues with dioxygenated rings has been described in our early study,^[21] all of which were promising building modules in the assembly of the newly designed compounds. Moreover, Lee et al.^[19] reported YKAs3003 (Scheme 2) to be a potent inhibitor

of pathogenic KAS III, performing well against various bacteria. Taken together, four novel compounds (1–3, and 5) were designed, and subsequently together with YKAs3003, a docking study was performed by using the CDOCKER algorithm.^[20] As default, each compound generally retained 10 preferential conformations, which would generate 50 poses in all. Next, we ranked all 50 poses by CDOCKER interaction energy, and the corresponding result is illustrated in Figure 2, showing the

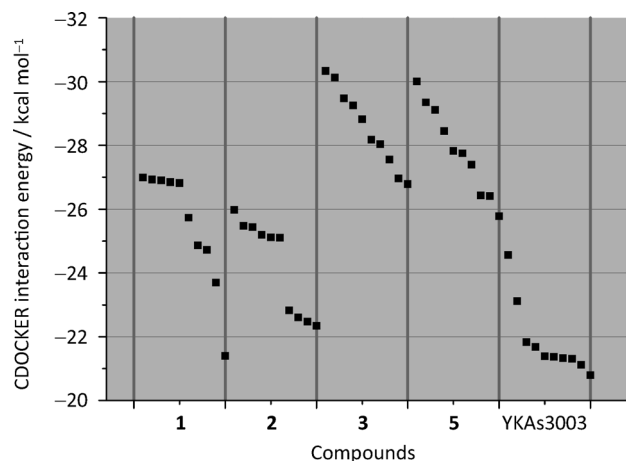


Figure 2. The CDOCKER interaction energy of the five active-like compounds: the lead compound YKAs3003 and four designed molecules (1–3, 5) docked into the active site of *E. coli* FabH receptor (PDB: 1HNJ)^[22]; the result shows that two compounds 3 and 5 (energy range generally from -30 kcal mol⁻¹ to -24 kcal mol⁻¹) perform better than the other three compounds.

energy values of the five small molecules in the range of -30 to -20 kcal mol⁻¹. Overall, compounds 3 and 5 gave better results than the other three compounds. Therefore, the dioxygenated rings that belonged to compound 1 and 2 were essentially ruled out, and the eight- and seven-membered rings located at the left position of the designed molecules were analyzed further. In order to determine which of the two dioxygenated rings the left bulk of the designed molecules was derived from, we attempted to build a FabH pharmacophore model based on the *E. coli* FabH protein complex that binds the substrate molecule malonyl-CoA.

In this construction process, seven small molecules (Figure 3) and malonyl-CoA were selected as the training set to generate the pharmacophore model with common feature. Since the Catalyst software is integrated into the Discovery Studio 3.1 platform,^[20] the pharmacophore generation method used could also be called “HipHop” derived from Catalyst. As previously described, we accomplished the docking study of these seven small compounds^[5] and chose the appropriate conformation before the pharmacophore model was generated. As to the training set, these compounds were classified into two groups: high active (6c–e, and substrate malonyl-CoA) and medium active (6a,b,f,g) according to their antimicrobial activity. In the treatment with HipHop, a “Principal” column that described the active level of the training set was added into the attribute of the compounds and the “Principal”

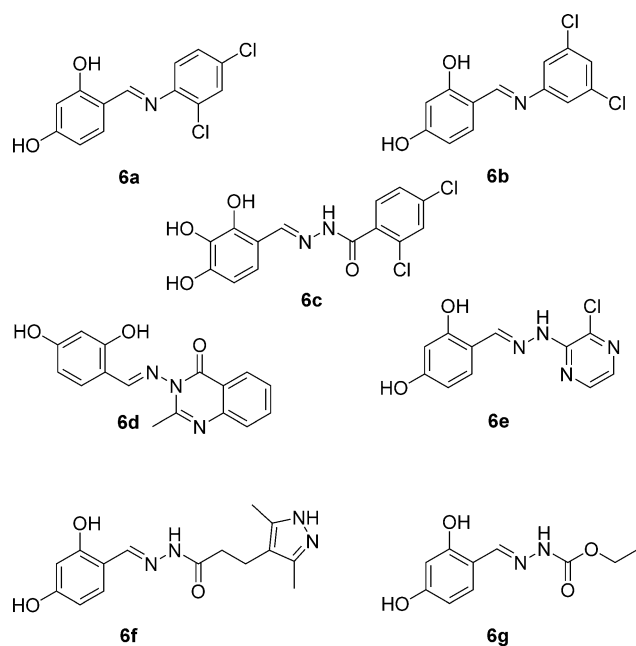


Figure 3. The training set, previously described compounds 6a–g,^[7] used by HipHop.

values of the high active group were set to two, whereas the medium active group was set to one. The next step was to pick up and refine the feature mapping derived from analysis of molecular docking conformation in the binding site. The instruction of common feature pharmacophore was implemented and 10 kinds of β -ketoacyl-ACP synthase III that ranked by RANK_score had been obtained, the first one of which was 46.712. As shown in Figure 4, this pharmacophore model, containing one ring and two acceptor features, could be selected as an effective tool to screen the docking poses of the five molecules (1–3, 5, and YKAs3003) in the further study.

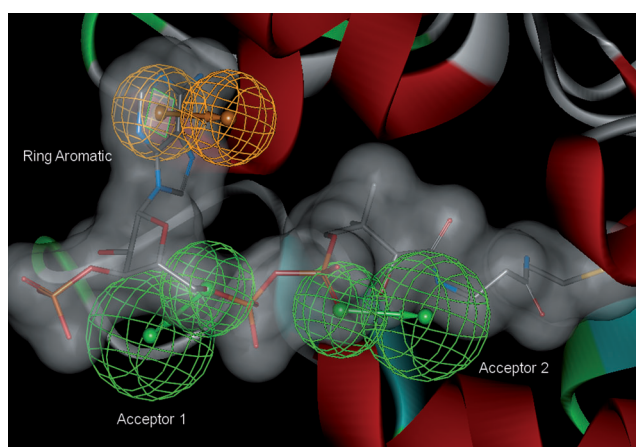


Figure 4. *E. coli* FabH protein (PDB: 1HNJ)^[22] receptor-oriented pharmacophore model. The procedures of construction based on the training set include: molecular docking of the training set molecules, and common feature pharmacophore generation by using the Discovery Studio 3.1.^[20] This map contains one aromatic ring and two acceptors.

All 50 poses from the five compounds could be collected into a small database, and clicking "Search, Screen and Profile", and inputting corresponding poses and finally the screening result including twenty matching poses would be obtained. The top five poses are listed in Table 1, and show that com-

Compd	Fit value ^[a]	Energy [kcal mol ⁻¹] ^[b]
YKAs3003	1.81484	-21.8319
5	1.57282	-28.4496
3	1.55467	-30.3326
2	1.46776	-25.4376
1	1.16376	-26.9283

[a] Results from screen of β -ketoacyl-ACP synthase III pharmacophore model. [b] CDOCKER interaction energy; results of the docking analysis.

pound 3 was slightly better than compound 5 in the "Fit value" evaluation, whereas 5 actually overmatched 3 in the interaction energy. Considering the high flexibility of the eight-membered ring derived from 3 and the high activity of FabH inhibitor with a seven-membered ring,^[21] compound 5 was selected as the designed molecule template. A series of Schiff bases (5–25) were designed, and their relative biological activities were investigated.

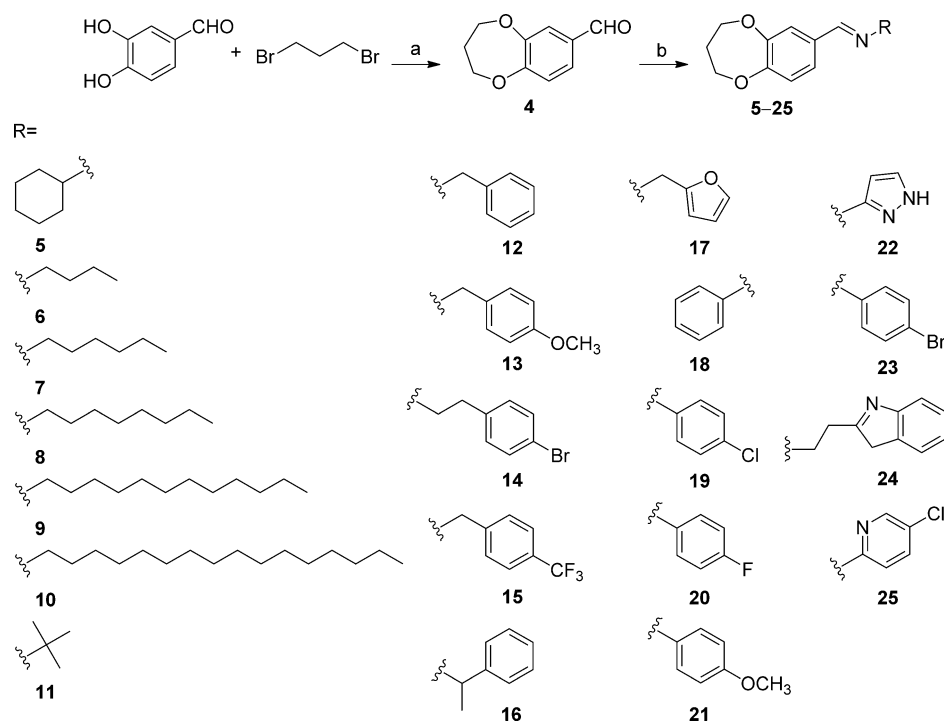
Chemistry

The synthetic route for preparing the targeted compounds 5–25 is outlined in Scheme 3. These compounds were synthesized from intermediate 4, which had been synthesized as previously described.^[21] In order to develop more effective antibiotics agents and conveniently discuss the different trends in structure–activity relationships (SARs) of the designed compounds, substituents on the right-hand part of compounds were replaced from previously used aliphatic amine groups (5–11) to aromatic amine groups (12–25). Thus, the designed compounds were prepared by a dehydration reaction of the intermediate aldehyde 4 with different amines dissolved in ethanol. The crude products were purified with flash chromatography, and compounds 5–25 were obtained with 80–95% yields. The struc-

tures of these compounds were fully characterized by spectroscopic methods and elemental analysis.

Biological activity

All synthesized compounds (5–25) were evaluated for antibacterial activity against the two Gram-negative bacterial strains, *E. coli* and *P. fluorescens*, and the two Gram-positive bacterial strains, *B. subtilis* and *S. aureus*, using an MTT (3-(4,5-dimethylthiazol-2-yl)-2,5-dihydroxybenzoic acid) assay. The minimum inhibitory concentrations (MIC) of these compounds against these bacteria are presented in Table 2. The antibacterial agent kanamycin B (positive control) was also screened under the same condition, and the results revealed that most of the small molecules exhibited a certain antibacterial activity. All tested compounds were divided into three groups according to their biological activity: high activity (8–10, 15, 23), medium activity (5, 7, 12–14, 17, 19, 20, 21, 24, 25), and low activity (6, 11, 16, 18, 22). All compounds in the high-activity group demonstrated excellent inhibitory activity against Gram-negative *E. coli* and *P. fluorescens*, and Gram-positive *B. subtilis* and *S. aureus*. Especially, compound 10 showed comparable activities to positive control kanamycin B (MIC = 3.89, 7.81, 7.81, and 3.89 μM^{-1} , respectively; Table 2). Most small molecules of the medium-activity group showed modest antibacterial activities against the four pathogenic strains, and the remaining compounds of the last group had little or no bioactivity for any strains.



Scheme 3. General synthesis of the Schiff base derivatives 5–21. Reagents and conditions: a) $\text{C}_2\text{S}_2\text{O}_3$, DMF, 70 °C, overnight; b) R-NH₂, EtOH, RT, overnight.

Compd ^[a]	Alog <i>P</i> ^[b]	MIC [$\mu\text{g mL}^{-1}$]			
		Gram-negative		Gram-positive	
		<i>E. coli</i>	<i>P. aeruginosa</i>	<i>B. subtilis</i>	<i>S. aureus</i>
5	3.556	25	50	50	> 100
6	3.026	>100	>100	>100	>100
7	3.939	12.5	12.5	50	25
8	4.851	3.13	6.25	6.25	12.5
9	6.676	3.13	3.13	6.25	6.25
10	8.501	1.56	3.13	3.13	1.56
11	2.629	50	>100	>100	>100
12	3.281	25	25	50	25
13	3.265	25	12.5	12.5	25
14	4.351	50	50	>100	50
15	4.223	6.25	12.5	25	12.5
16	3.659	>100	>100	>100	>100
17	2.463	50	50	50	100
18	3.274	>100	>100	>100	>100
19	3.939	12.5	12.5	25	12.5
20	3.480	50	25	50	50
21	3.258	50	50	50	100
22	2.257	>100	>100	>100	>100
23	4.023	6.25	6.25	3.13	3.13
24	3.234	25	50	25	25
25	3.327	12.5	25	12.5	25
Kanamycin B	-7.144	3.13	3.13	1.56	1.56

[a] The compounds tested for antibacterial activity are consistent with the description in the Experimental Section. [b] Calculated with Discovery studio 3.1.^[20]

In order to describe the SARs of these compounds, this series was classified into two groups: compounds with aliphatic amine side chains (5–11) and those with aromatic amine substituents (12–25). Compared with the aromatic group, the aliphatic group could contribute more to the antibiotic activity of the compounds, maybe due to their hydrophobic properties. Although compounds 6 and 11 exhibited poor activity, the reason for this may lie in the steric clash located in the binding site of the target protein rather than in the hydrophobic nature of the aliphatic amine substituents. Moreover, increasing the length of the aliphatic chain seems to enhance the potency of compounds as seen in the MIC values from compound 6 to 10 (see Table 2). Correspondingly, the predicted lipophilicity (Alog *P*) values of these four molecules rise in the same order. In the aromatic group, some compounds possessed effective antibacterial activities and others maintained lower activities, which indicates that the two factors (substituents on the benzene ring, and length of the linker between the benzene ring and N atom) affect their antibacterial activity. As shown in Table 2, one- or two-carbon-atom gaps between the benzene ring and N atom were favorable for the relative biological activity when comparing compounds 12–15 with 17–21. However, compound 23 represents an exception, probably because the bromine substituent could make up for loss of activity caused by the length of the linker. As to the substituent of the benzene ring, trifluoromethyl performed better than other moieties (compound 15). The last noticeable discovery from compounds 24 and 25 was that the heterocycle replacing the benzene ring was another strategy to explore better antibacterial agents.

The *E. coli* FabH inhibitory potencies of the synthetic compounds with potent antibacterial activities (6–10, 13, 15, 23–25) were examined, and the results are listed in Table 3. All

Compd ^[a]	<i>E. coli</i> FabH IC ₅₀ [μM]	Hemolysis LC ^[b] [mg mL^{-1}]	PSA ^[c] [\AA^2]	Alog <i>P</i> ^[c]
6	9.3	>10	32.43	2.923
7	7.4	>10	30.82	3.939
8	3.3	>10	30.82	4.851
9	2.1	>10	30.82	6.676
10	1.6	>10	30.82	8.501
13	15.5	>10	41.66	3.161
15	6.8	>10	32.43	4.12
23	5.9	>10	30.82	4.023
24	12.7	>10	44.79	3.13
25	4.4	>10	43.71	3.327

[a] The compounds tested for antibacterial activity are consistent with the description in the Experimental Section. [b] Lytic concentration 30%. [c] Molecular polar surface area (PSA); calculated with Discovery studio 3.1.^[20]

tested compounds showed potent *E. coli* FabH inhibition, and particularly compounds 8–10 with aliphatic substituents showed considerable inhibitory activities ($\text{IC}_{50} < 4 \mu\text{M}$). With the length of the aliphatic chain from compound 7 to 10, the inhibitory activities increased, and this result supports the potent antibacterial activities of 10 being the most potent FabH inhibitor. Compounds 6, 13 and 24 actually exhibited moderate inhibitory activities but very poor antibacterial activities. This disparity could be explained by their Alog *P* values (Table 3). Compared with the other tested compounds, 6, 13 and 24 have lower Alog *P* values, which could indicate these small molecules do not easily penetrate the bacterial cell membrane. The molecular polar surface areas (PSA) of these compounds were in the range of 30–44 \AA^2 , and therefore, this molecular property cannot significantly account for the results obtained. In summary, the results of the *E. coli* FabH inhibitory activity of the test compounds described above generally corresponded to the SARs of their antibacterial activities. This demonstrates that the potent antibacterial activities of the selected compounds are probably correlated to their FabH inhibitory activities.

With the aim to determine the interaction binding mode between the target protein and small molecules, molecular docking of the most active compound 10 and *E. coli* FabH was performed on the binding model based on the *E. coli* FabH–CoA complex structure (PDB: 1HNJ).^[22] The corresponding result is shown in Figure 5, which is composed of three interaction maps. The docking study was performed using the CDOCKER protocol.^[20] The 3D optimal conformation and the 2D diagram interacting with the FabH active site are presented in Figure 5a and b, respectively. The two amino acid residues Arg151 and Trp32 each form π – π interactions with compound 10, making them vital for the stabilization of its binding mode. Figure 5c shows the LUDI interaction map of the binding pocket inside

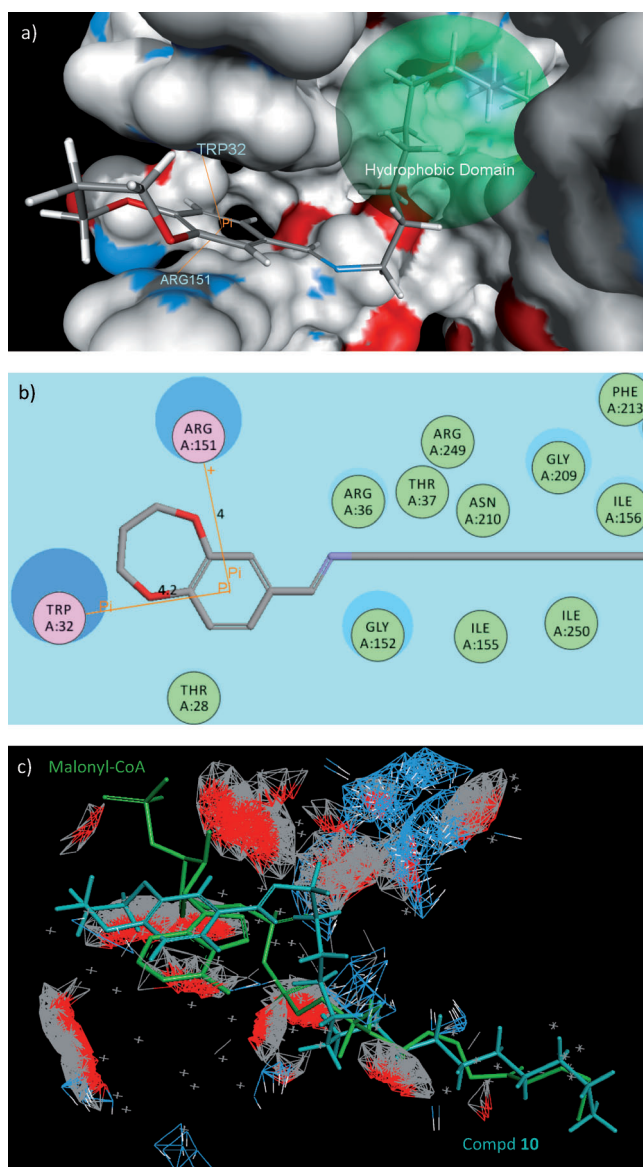


Figure 5. Three interaction maps of compound **10** derived from the docking studies that display: a) the 3D diagram, b) the 2D diagram, c) the Ludi interaction map. In panels a and b, the models predict the formation of a π - π interaction with residue Arg151 and a π -cation bond with residue Trp32, and as such, the aliphatic chain of compound **10** is easily inserted into the hydrophobic domain in the active center, which could favor binding. The interaction map shown in panel c is directly involved in the pharmacophore analysis of the ligand-protein complex (PDB: 1HNJ), which could search three basic features in the protein active pocket (hydrogen bond acceptor labeled as red sticks, hydrogen bond donor labeled as blue sticks, and the hydrophobic site labeled as gray point). The figure shows a defined spatial network in which compound **10** and the natural substrate malonyl-CoA can both circumvent the hydrophobic points and match the corresponding donor or acceptor sites well.

the protein receptor, mainly depicting the interaction environment around the existing substrate malonyl-CoA. Strikingly, the molecular binding mode demonstrates that compound **10** could mimic the original crystal conformation of substrate malonyl-CoA. This supports the understanding of the most active

compound **10**. In addition, the assay data of *E. coli* FabH inhibitory activity also indicates that compound **10** is a potential inhibitor of *E. coli* FabH with potent antibacterial activity.

Conclusions

In this paper, 21 novel Schiff base derivatives (**5–25**) were synthesized and for the first time evaluated for *E. coli* FabH inhibitory activity as antibacterial agents. Within this research, several compounds with potent and selective anti-Gram-negative bacteria activities were obtained. Compounds **8–10**, and **25** exhibited excellent activities against Gram-negative *E. coli* and *P. aeruginosa*. Particularly, compound **10** showed the most potent *E. coli* FabH inhibitory activity with an IC_{50} value of $1.6 \mu\text{M}$, which was compared with the positive control, kanamycin B. Molecular docking simulation was performed to position compound **10** into the *E. coli* FabH active site in order to determine the probable binding conformation. Based on the data obtained in this study, we conclude that compound **10** is the *E. coli* FabH inhibitor most deserving of further research as a potential antibiotic. Moreover, the development of similar novel compounds based on the structure of compound **3** will be investigated in future studies.

Experimental Section

Chemistry

General: All chemicals (reagent grade) were purchased from Sigma-Aldrich. Separation of the compounds by column chromatography was carried out with silica gel 60 (200–300 mesh ASTM, Merck). The quantity of silica gel used was 50–100 times the weight charged on the column. Then, the eluates were monitored using thin-layer chromatography (TLC). Melting points (mp) were determined on a XT4 MP apparatus (Taike Corp., Beijing, China). ESI mass spectra (MS) were obtained on a Mariner System 5304 mass spectrometer, and ^1H and ^{13}C NMR spectra were recorded on a Bruker DPX 400 spectrometer. Elemental analyses were performed on a Heraeus CHN-O-Rapid instrument and were within $\pm 0.4\%$ of the theoretical values.

3,4-dihydro-2H-benzo[b][1,4]dioxepine-7-carbaldehyde (4): The synthesis was performed as previously described.^[21] 3,4-Dihydroxybenzaldehyde (0.716 g, 5.2 mmol) and Cs_2CO_3 (3.389 g, 10.4 mmol) were added to a 25 mL round flask. Dry DMF (8 mL), and 1,3-dibromopropane (2.1 g, 10.4 mmol) was added, and the reaction mixture was heated to 70°C overnight. After cooling to RT and filtration (Celite), the filtrate was concentrated in vacuo. The crude product was purified by column chromatography (SiO_2 , EtOAc/hexane), and compound **4** was obtained as a colorless oil (814 mg, 88%): $R_f=0.6$ (EtOAc/hexane, 1:4); ^1H NMR (400 MHz, CDCl_3): $\delta=9.85$ (s, 1 H), 7.47 (dd, $J=7.2, 1.8$ Hz, 2 H), 7.06 (m, 1 H), 4.36 (m, 2 H), 4.30 (t, $J=5.9$ Hz, 2 H), 2.26 ppm (m, 2 H); ^{13}C NMR (100 MHz, CDCl_3): $\delta=190.5, 156.4, 151.0, 131.9, 125.4, 122.7, 121.8, 70.3, 70.2, 30.7$ ppm; MS (ESI): m/z 179.2 $[M+H]^+$; Anal. calcd for $\text{C}_{10}\text{H}_{10}\text{O}_3$: C 67.41, H 5.66, O 26.94, found: C 67.32, H 5.68, O 26.96.

(E)-N-((3,4-dihydro-2H-benzo[b][1,4]dioxepin-7-yl)methylene)cyclohexanamine (5): Compound **4** (535 mg, 3 mmol) was dissolved in MeOH (3 mL), and cyclohexanamine (3.6 mmol, 357 mg) was added. The reaction mixture was stirred at RT overnight. The sol-

vent was removed in vacuo, and the crude product was purified by column chromatography (Neutral Al₂O₃, EtOAc/hexane) to give compound **5** as a yellow solid (700 mg, 90%); *R*_f = 0.6 (EtOAc/hexane, 1:4); mp: 68.0–68.9 °C; ¹H NMR (400 MHz, CDCl₃): δ = 8.19 (s, 1H), 7.36 (d, *J* = 2.0 Hz, 1H), 7.28 (m, 1H), 6.97 (d, *J* = 8.2 Hz, 1H), 4.23 (m, 4H), 3.15 (m, 1H), 2.20 (m, 2H), 1.82 (m, 2H), 1.68 (m, 2H), 1.56 (m, 2H), 1.31 ppm (m, 4H); ¹³C NMR (100 MHz, CDCl₃): δ = 157.5, 153.1, 151.1, 132.3, 123.3, 121.5, 121.1, 70.4, 70.4, 69.8, 34.4, 31.5, 25.7, 24.8 ppm; MS (ESI): *m/z* 260.3 [M+H]⁺; Anal. calcd for C₁₆H₂₁NO₂: C 74.10, H 8.16, N 5.40, found: C 74.10, H 8.16, N 5.40.

Compounds **6–25** were synthesized as described for compound **5** (see above) with the corresponding amine.

(E)-N-((3,4-dihydro-2H-benzo[b][1,4]dioxepin-7-yl)methylene)butan-1-amine (6): Compound **6** was obtained as a yellow oil (558 mg, 94%); *R*_f = 0.6 (EtOAc/hexane, 1:5); ¹H NMR (400 MHz, CDCl₃): δ = 8.15 (s, 1H), 7.35 (d, *J* = 2.0 Hz, 1H), 7.28 (m, 1H), 6.98 (d, *J* = 8.2 Hz, 1H), 4.24 (m, 4H), 3.57 (m, 2H), 2.21 (m, 2H), 1.66 (m, 2H), 1.37 (m, 2H), 0.94 ppm (t, *J* = 7.4 Hz, 3H); ¹³C NMR (100 MHz, CDCl₃): δ = 159.6, 153.2, 151.1, 132.0, 123.2, 121.6, 121.1, 70.4, 61.3, 33.0, 31.5, 20.4, 13.9 ppm; MS (ESI): *m/z* 234.3 [M+H]⁺; Anal. calcd for C₁₄H₁₉NO₂: C 72.07, H 8.21, N 6.00, found: C 72.23, H 8.11, N 6.07.

(E)-N-((3,4-dihydro-2H-benzo[b][1,4]dioxepin-7-yl)methylene)hexan-1-amine (7): Compound **7** was obtained as a yellow oil (408 mg, 92%); *R*_f = 0.6 (EtOAc/hexane, 1:5); ¹H NMR (400 MHz, CDCl₃): δ = 8.13 (s, 1H), 7.34 (d, *J* = 2.0 Hz, 1H), 7.27 (m, 1H), 6.96 (d, *J* = 8.2 Hz, 1H), 4.21 (m, 4H), 3.54 (dd, *J* = 10.1, 3.9 Hz, 2H), 2.18 (m, 2H), 1.65 (m, 2H), 1.31 (t, *J* = 7.1 Hz, 6H), 0.87 ppm (t, *J* = 6.7 Hz, 3H); ¹³C NMR (100 MHz, CDCl₃): δ = 159.5, 153.1, 151.1, 132.0, 123.2, 121.5, 121.1, 70.4, 61.6, 31.7, 31.5, 30.9, 27.0, 22.6, 14.1 ppm; MS (ESI): *m/z* 262.3 [M+H]⁺; Anal. calcd for C₁₆H₂₃NO₂: C 73.53, H 8.87, N 5.36, found: C 73.92, H 9.07, N 4.93.

(E)-N-((3,4-dihydro-2H-benzo[b][1,4]dioxepin-7-yl)methylene)octan-1-amine (8): Compound **8** was obtained as a yellow oil (294 mg, 94%); *R*_f = 0.7 (EtOAc/hexane, 1:8); ¹H NMR (400 MHz, CDCl₃): δ = 8.13 (s, 1H), 7.34 (d, *J* = 2.0 Hz, 1H), 7.27 (m, 1H), 6.96 (d, *J* = 8.2 Hz, 1H), 4.22 (m, 4H), 3.55 (m, 2H), 2.19 (dd, *J* = 11.4, 5.7 Hz, 2H), 1.66 (m, 2H), 1.29 (m, 10H), 0.87 ppm (t, *J* = 6.8 Hz, 3H); ¹³C NMR (100 MHz, CDCl₃): δ = 159.5, 153.1, 151.1, 132.0, 123.2, 121.5, 121.1, 70.4, 61.6, 31.9, 31.5, 31.0, 29.4, 29.3, 27.3, 22.7, 14.1 ppm; MS (ESI): *m/z* 290.4 [M+H]⁺; Anal. calcd for C₁₈H₂₇NO₂: C 74.70, H 9.40, N 4.84, found: C 74.61, H 9.48, N 4.92.

(E)-N-((3,4-dihydro-2H-benzo[b][1,4]dioxepin-7-yl)methylene)dodecan-1-amine (9): Compound **9** was obtained as a yellow oil (331 mg, 93%); *R*_f = 0.8 (EtOAc/hexane, 1:8); ¹H NMR (400 MHz, CDCl₃): δ = 8.14 (s, 1H), 7.35 (d, *J* = 2.0 Hz, 1H), 7.28 (m, 1H), 6.97 (d, *J* = 8.2 Hz, 1H), 4.23 (m, 4H), 3.55 (m, 2H), 2.19 (m, 2H), 1.66 (m, 2H), 1.29 (m, 18H), 0.88 ppm (t, *J* = 6.8 Hz, 3H); ¹³C NMR (100 MHz, CDCl₃): δ = 159.5, 153.1, 151.1, 132.0, 123.2, 121.5, 121.1, 70.4, 61.6, 31.9, 31.5, 31.0, 29.7, 29.6, 29.6, 29.5, 29.3, 27.3, 22.7, 14.1 ppm; MS (ESI): *m/z* 346.5 [M+H]⁺; Anal. calcd for C₂₂H₃₅NO₂: C 76.47, H 10.21, N 4.05, found: C 76.63, H 11.33, N 3.97.

(E)-N-((3,4-dihydro-2H-benzo[b][1,4]dioxepin-7-yl)methylene)hexadecan-1-amine (10): Compound **10** was obtained as a pale yellow solid (365 mg, 95%); *R*_f = 0.7 (EtOAc/hexane, 1:10); mp: 51.0–52.0 °C; ¹H NMR (400 MHz, CDCl₃): δ = 8.15 (s, 1H), 7.35 (d, *J* = 2.0 Hz, 1H), 7.28 (m, 1H), 6.98 (d, *J* = 8.2 Hz, 1H), 4.24 (m, 4H), 3.56 (m, 2H), 2.21 (dd, *J* = 11.4, 5.7 Hz, 2H), 1.67 (m, 2H), 1.29 (m, 26H),

0.88 ppm (t, *J* = 6.8 Hz, 3H); ¹³C NMR (100 MHz, CDCl₃): δ = 159.5, 153.1, 151.1, 132.0, 123.2, 121.6, 121.1, 70.4, 61.7, 31.9, 31.5, 31.0, 29.7, 29.6, 29.5, 29.4, 27.4, 22.7, 14.1 ppm; MS (ESI): *m/z* 402.6 [M+H]⁺; Anal. calcd for C₂₆H₄₃NO₂: C 77.75, H 10.79, N 3.49, found: C 77.38, H 10.62, N 3.84.

(E)-N-((3,4-dihydro-2H-benzo[b][1,4]dioxepin-7-yl)methylene)-2-methylpropan-2-amine (11): Compound **11** was obtained as a yellow oil (270 mg, 91%); *R*_f = 0.6 (EtOAc/hexane, 1:6); ¹H NMR (400 MHz, CDCl₃): δ = 8.15 (s, 1H), 7.35 (d, *J* = 2.0 Hz, 1H), 7.28 (m, 1H), 6.98 (d, *J* = 8.2 Hz, 1H), 4.24 (m, 4H), 2.21 (dd, *J* = 11.4, 5.7 Hz, 2H), 1.35 ppm (s, 9H); ¹³C NMR (100 MHz, CDCl₃): δ = 159.5, 153.1, 151.1, 132.0, 123.2, 121.6, 121.1, 70.4, 31.5 ppm; MS (ESI): *m/z* 334.1 [M+H]⁺; Anal. calcd for C₁₄H₁₉NO₂: C 72.07, H 8.21, N 6.00, found: C 72.07, H 8.21, N 6.00.

(E)-N-((3,4-dihydro-2H-benzo[b][1,4]dioxepin-7-yl)methylene)-1-phenylmethanamine (12): Compound **12** was obtained as a yellow oil (454 mg, 86%); *R*_f = 0.6 (EtOAc/hexane, 1:4); ¹H NMR (400 MHz, CDCl₃): δ = 8.29 (s, 1H), 7.45 (t, *J* = 5.4 Hz, 1H), 7.36 (m, 5H), 7.28 (dd, *J* = 7.0, 2.5 Hz, 1H), 7.01 (dd, *J* = 8.2, 1.6 Hz, 1H), 4.80 (s, 2H), 4.25 (m, 4H), 2.20 ppm (m, 2H); ¹³C NMR (100 MHz, CDCl₃): δ = 160.9, 153.5, 151.2, 139.5, 131.8, 128.5, 128.0, 127.0, 123.6, 121.6, 121.4, 70.4, 64.9, 31.5 ppm; MS (ESI): *m/z* 268.3 [M+H]⁺; Anal. calcd for C₁₇H₁₇NO₂: C 76.38, H 6.41, N 5.24, found: C 76.42, H 6.62, N 5.07.

(E)-N-((3,4-dihydro-2H-benzo[b][1,4]dioxepin-7-yl)methylene)-1-(4-methoxyphenyl)methanamine (13): Compound **13** was obtained as a yellow solid (290 mg, 90%); *R*_f = 0.7 (EtOAc/hexane, 1:4); mp: 134.4–135.2 °C; ¹H NMR (400 MHz, CDCl₃): δ = 8.36 (s, 1H), 7.56 (s, 1H), 7.48 (dd, *J* = 8.3, 1.9 Hz, 1H), 7.20 (d, *J* = 8.1 Hz, 2H), 7.14 (d, *J* = 8.1 Hz, 2H), 7.05 (d, *J* = 8.2 Hz, 1H), 4.29 (m, 4H), 2.39 (s, 3H), 2.24 ppm (m, 4H); ¹³C NMR (100 MHz, CDCl₃): δ = 158.4, 153.9, 151.2, 149.5, 135.6, 132.0, 129.8, 124.2, 121.8, 120.8, 115.3, 70.4, 70.4, 31.4, 21.0, 20.5 ppm; MS (ESI): *m/z* 298.4 [M+H]⁺; Anal. calcd for C₁₈H₁₉NO₃: C 72.71, H 6.44, N 4.71, found: C 72.53, H 6.79, N 4.47.

(E)-2-(4-bromophenyl)-N-((3,4-dihydro-2H-benzo[b][1,4]dioxepin-7-yl)methylene)ethanamine (14): Compound **14** was obtained as a white solid (522 mg, 91%); *R*_f = 0.7 (EtOAc/hexane, 1:4); mp: 141.7–142.5 °C; ¹H NMR (400 MHz, CDCl₃): δ = 8.03 (s, 1H), 7.39 (m, 2H), 7.33 (d, *J* = 2.0 Hz, 1H), 7.25 (m, 1H), 7.10 (d, *J* = 8.4 Hz, 2H), 6.98 (d, *J* = 8.2 Hz, 1H), 4.26 (m, 4H), 3.79 (m, 2H), 2.95 (t, *J* = 7.2 Hz, 2H), 2.21 ppm (m, 2H); ¹³C NMR (100 MHz, CDCl₃): δ = 160.5, 153.3, 151.1, 139.0, 131.7, 131.4, 130.8, 123.3, 121.6, 121.1, 119.9, 70.4, 62.7, 36.9, 31.5 ppm; MS (ESI): *m/z* 361.3 [M+H]⁺; Anal. calcd for C₁₈H₁₈BrNO₂: C 60.01, H 5.04, N 3.89, found: C 60.33, H 5.36, N 4.01.

N-((3,4-dihydro-2H-benzo[b][1,4]dioxepin-7-yl)methylene)-1-(4-(trifluoromethyl)phenyl)methanamine (15): Compound **15** was obtained as a yellow solid (546 mg, 89%); *R*_f = 0.5 (EtOAc/hexane, 1:4); mp: 136.2–137.8 °C; ¹H NMR (400 MHz, CDCl₃): δ = 8.30 (s, 1H), 7.60 (d, *J* = 8.1 Hz, 2H), 7.46 (m, 3H), 7.36 (dd, *J* = 8.3, 2.0 Hz, 1H), 7.01 (d, *J* = 8.2 Hz, 1H), 4.82 (s, 2H), 4.26 (m, 4H), 2.21 ppm (m, 2H); ¹³C NMR (100 MHz, CDCl₃): δ = 161.6, 153.7, 151.2, 143.8, 131.5, 128.1, 125.4, 125.4, 125.3, 123.7, 121.7, 121.3, 70.4, 70.4, 64.2, 31.4 ppm; MS (ESI): *m/z* 336.3 [M+H]⁺; Anal. calcd for C₁₈H₁₆F₃NO₂: C 64.47, H 4.81, N 4.18, found: C 64.62, H 4.52, N 4.39.

(R,E)-N-((3,4-dihydro-2H-benzo[b][1,4]dioxepin-7-yl)methylene)-1-phenylethanamine (16): Compound **16** was obtained as

a yellow oil (477 mg, 92%); $R_f=0.6$ (EtOAc/hexane, 1:4); $^1\text{H NMR}$ (400 MHz, CDCl_3): $\delta=8.26$ (s, 1H), 7.43 (dd, $J=9.1, 4.7$ Hz, 3H), 7.35 (m, 3H), 7.25 (m, 1H), 6.98 (d, $J=8.2$ Hz, 1H), 4.51 (q, $J=6.6$ Hz, 1H), 4.25 (m, 4H), 2.21 (m, 2H), 1.58 ppm (t, $J=5.2$ Hz, 3H); $^{13}\text{C NMR}$ (100 MHz, CDCl_3): $\delta=158.3, 153.3, 151.1, 145.4, 132.1, 128.6, 128.4, 126.8, 126.6, 123.6, 121.5, 121.2, 70.4, 69.6, 31.5, 24.9$ ppm; MS (ESI): m/z 282.4 $[M+H]^+$; Anal. calcd for $\text{C}_{18}\text{H}_{19}\text{NO}_2$: C 76.84, H 6.81, N 4.98, found: C 76.99, H 6.72, N 4.65.

(E)-N-((3,4-dihydro-2H-benzo[b][1,4]dioxepin-7-yl)methylene)-1-(furan-2-yl)methanamine (17): Compound 17 was obtained as a yellow solid (364 mg, 84%); $R_f=0.5$ (EtOAc/hexane, 1:4); mp: 154.2–155.0 °C; $^1\text{H NMR}$ (400 MHz, CDCl_3): $\delta=8.22$ (s, 1H), 7.39 (dd, $J=10.0, 1.5$ Hz, 2H), 7.33 (dd, $J=8.3, 2.0$ Hz, 1H), 6.98 (d, $J=8.3$ Hz, 1H), 6.34 (dd, $J=3.0, 1.9$ Hz, 1H), 6.25 (d, $J=3.0$ Hz, 1H), 4.73 (s, 2H), 4.23 (m, 4H), 2.19 ppm (m, 2H); $^{13}\text{C NMR}$ (100 MHz, CDCl_3): $\delta=161.9, 153.5, 152.5, 151.1, 142.1, 131.5, 123.6, 121.6, 121.4, 110.4, 107.4, 70.4, 57.1, 31.4$ ppm; MS (ESI): m/z 258.3 $[M+H]^+$; Anal. calcd for $\text{C}_{15}\text{H}_{15}\text{NO}_3$: C 70.02, H 5.88, N 5.44, found: C 70.12, H 5.94, N 5.421.

(E)-N-((3,4-dihydro-2H-benzo[b][1,4]dioxepin-7-yl)methylene)aniline (18): Compound 18 was obtained as a yellow solid (548 mg, 91%); $R_f=0.5$ (EtOAc/hexane, 1:4); mp: 92.5–93.4 °C; $^1\text{H NMR}$ (400 MHz, CDCl_3): $\delta=8.29$ (s, 1H), 7.45 (t, $J=5.4$ Hz, 1H), 7.36 (m, 5H), 7.28 (dd, $J=7.0, 2.5$ Hz, 1H), 7.01 (dd, $J=8.2, 1.6$ Hz, 1H), 4.25 (m, 4H), 2.20 ppm (m, 2H); $^{13}\text{C NMR}$ (100 MHz, CDCl_3): $\delta=160.9, 153.5, 151.2, 139.5, 131.8, 128.5, 128.0, 127.0, 123.6, 121.6, 121.4, 70.4, 31.5$ ppm; MS (ESI): m/z 254.3 $[M+H]^+$; Anal. calcd for $\text{C}_{16}\text{H}_{15}\text{NO}_2$: C 75.87, H 5.97, N 5.53, found: C 75.66, H 5.83, N 5.72.

(E)-4-chloro-N-((3,4-dihydro-2H-benzo[b][1,4]dioxepin-7-yl)methylene)aniline (19): Compound 19 was obtained as a yellow solid (390 mg, 88%); $R_f=0.5$ (EtOAc/hexane, 1:4); mp: 101.2–101.7 °C; $^1\text{H NMR}$ (400 MHz, CDCl_3): $\delta=8.31$ (s, 1H), 7.54 (d, $J=2.0$ Hz, 1H), 7.47 (dd, $J=8.3, 2.0$ Hz, 1H), 7.34 (m, 2H), 7.13 (m, 2H), 7.04 (d, $J=8.3$ Hz, 1H), 4.29 (m, 4H), 2.24 ppm (m, 2H); $^{13}\text{C NMR}$ (100 MHz, CDCl_3): $\delta=159.5, 154.2, 151.2, 150.5, 131.3, 129.2, 124.4, 122.2, 121.9, 121.8, 116.2, 70.4, 70.4, 31.3$ ppm; MS (ESI): m/z 288.7 $[M+H]^+$; Anal. calcd for $\text{C}_{16}\text{H}_{14}\text{ClNO}_2$: C 66.79, H 4.90, N 4.87, found: C 66.88, H 4.97, N 4.56.

(E)-N-((3,4-dihydro-2H-benzo[b][1,4]dioxepin-7-yl)methylene)-4-fluoroaniline (20): Compound 20 was obtained as a yellow solid (382 mg, 85%); $R_f=0.5$ (EtOAc/hexane, 1:4); mp: 101.7–109.8 °C; $^1\text{H NMR}$ (400 MHz, CDCl_3): $\delta=8.31$ (s, 1H), 7.53 (d, $J=2.0$ Hz, 1H), 7.46 (dd, $J=8.3, 2.0$ Hz, 1H), 7.34 (m, 2H), 7.12 (m, 2H), 7.04 (d, $J=8.3$ Hz, 1H), 4.29 (m, 4H), 2.24 ppm (p, $J=5.7$ Hz, 2H); $^{13}\text{C NMR}$ (100 MHz, CDCl_3): $\delta=159.5, 154.2, 151.2, 150.6, 131.5, 131.2, 129.2, 124.3, 122.2, 121.9, 121.8, 70.4, 70.4, 31.3$ ppm; MS (ESI): m/z 272.3 $[M+H]^+$; Anal. calcd for $\text{C}_{16}\text{H}_{14}\text{FNO}_2$: C 70.84, H 5.20, N 5.16, found: C 70.61, H 5.28, N 5.33.

(E)-N-((3,4-dihydro-2H-benzo[b][1,4]dioxepin-7-yl)methylene)-4-methoxyaniline (21): Compound 21 was obtained as a yellow solid (440 mg, 90%); $R_f=0.6$ (EtOAc/hexane, 1:4); mp: 108.5–109.1 °C; $^1\text{H NMR}$ (400 MHz, CDCl_3): $\delta=8.36$ (s, 1H), 7.53 (d, $J=2.0$ Hz, 1H), 7.46 (dd, $J=8.3, 2.0$ Hz, 1H), 7.21 (m, 2H), 7.03 (d, $J=8.3$ Hz, 1H), 6.93 (m, 2H), 4.28 (m, 4H), 3.83 (s, 3H), 2.23 ppm (m, 2H); $^{13}\text{C NMR}$ (100 MHz, CDCl_3): $\delta=158.2, 157.3, 153.7, 151.2, 145.0, 132.1, 124.0, 122.1, 121.7, 121.6, 114.4, 70.4, 55.5, 31.4$ ppm; MS (ESI): m/z 284.3 $[M+H]^+$; Anal. calcd for $\text{C}_{17}\text{H}_{17}\text{NO}_3$: C 72.07, H 6.05, N 4.94, found: C 72.18, H 6.24, N 4.59.

(E)-N-((3,4-dihydro-2H-benzo[b][1,4]dioxepin-7-yl)methylene)-1H-pyrazol-3-amine (22): Compound 22 was obtained as a white solid (370 mg, 81%); $R_f=0.3$ (EtOAc/hexane, 1:4); mp: 89.4–90.8 °C; $^1\text{H NMR}$ (400 MHz, CDCl_3): $\delta=8.61$ (s, 2H), 8.55 (s, 1H), 7.44 (d, $J=2.0$ Hz, 1H), 7.37 (dd, $J=8.3, 2.0$ Hz, 1H), 6.99 (d, $J=8.3$ Hz, 1H), 4.27 (m, 4H), 2.21 ppm (m, 2H); $^{13}\text{C NMR}$ (100 MHz, CDCl_3): $\delta=156.3, 155.0, 151.2, 138.3, 126.6, 124.5, 122.1, 121.7, 70.4, 70.3, 31.0$ ppm; MS (ESI): m/z 244.3 $[M+H]^+$; Anal. calcd for $\text{C}_{13}\text{H}_{13}\text{N}_3\text{O}_2$: C 64.19, H 5.39, N 17.27, Found: C 64.38, H 5.27, N 17.22.

(E)-4-bromo-N-((3,4-dihydro-2H-benzo[b][1,4]dioxepin-7-yl)methylene)aniline (23): Compound 23 obtained as a yellow solid (420 mg, 87%); $R_f=0.5$ (EtOAc/hexane, 1:4); mp: 102.3–103.4 °C; $^1\text{H NMR}$ (400 MHz, CDCl_3): $\delta=8.29$ (s, 1H), 7.53 (d, $J=2.0$ Hz, 1H), 7.46 (m, 3H), 7.05 (t, $J=8.9$ Hz, 3H), 4.28 (m, 4H), 2.23 ppm (m, 2H); $^{13}\text{C NMR}$ (100 MHz, CDCl_3): $\delta=159.6, 154.2, 151.2, 151.0, 132.2, 131.5, 124.4, 122.6, 121.9, 121.8, 119.1, 119.1, 70.4, 31.3$ ppm; MS (ESI): m/z 333.2 $[M+H]^+$; Anal. calcd for $\text{C}_{16}\text{H}_{14}\text{BrNO}_2$: C 57.85, H 4.25, N 4.22, found: C 57.85, H 4.25, N 4.22.

(E)-N-((3,4-dihydro-2H-benzo[b][1,4]dioxepin-7-yl)methylene)-2-(3H-indol-2-yl)ethanamine (24): Compound 24 was obtained as a white solid (450 mg, 82%); $R_f=0.4$ (EtOAc/hexane, 1:4); mp: 168.7–169.3 °C; $^1\text{H NMR}$ (400 MHz, CDCl_3): $\delta=8.04$ (d, $J=12.8$ Hz, 2H), 7.67 (d, $J=7.7$ Hz, 1H), 7.35 (d, $J=6.3$ Hz, 2H), 7.28 (d, $J=10.6$ Hz, 1H), 7.20 (t, $J=7.3$ Hz, 1H), 7.13 (t, $J=7.3$ Hz, 1H), 6.99 (m, 2H), 4.25 (m, 4H), 3.91 (t, $J=7.1$ Hz, 2H), 3.16 (t, $J=7.2$ Hz, 2H), 2.21 ppm (m, 2H); $^{13}\text{C NMR}$ (100 MHz, CDCl_3): $\delta=160.4, 153.3, 151.2, 136.3, 131.9, 127.6, 123.4, 122.3, 121.9, 121.6, 121.2, 119.2, 119.0, 114.0, 111.2, 70.5, 61.9, 31.5, 27.0$ ppm; MS (ESI): m/z 321.4 $[M+H]^+$; Anal. calcd for $\text{C}_{20}\text{H}_{20}\text{N}_2\text{O}_2$: C 74.98, H 6.29, N 8.74, found: C 75.04, H 6.33, N 8.51.

(E)-5-chloro-N-((3,4-dihydro-2H-benzo[b][1,4]dioxepin-7-yl)methylene)pyridin-2-amine (25): Compound 25 was obtained as a white solid (334 mg, 87%); $R_f=0.4$ (EtOAc/hexane, 1:4); mp: 121.0–121.4 °C; $^1\text{H NMR}$ (400 MHz, CDCl_3): $\delta=9.43$ (s, 1H), 7.60 (d, $J=1.8$ Hz, 1H), 7.54 (m, 3H), 7.25 (m, 1H), 7.02 (d, $J=8.3$ Hz, 1H), 4.30 (m, 4H), 2.24 ppm (m, 2H); $^{13}\text{C NMR}$ (100 MHz, CDCl_3): $\delta=164.9, 155.6, 155.3, 151.1, 130.4, 125.7, 122.8, 122.6, 122.0, 115.0, 70.3, 70.3, 31.0$ ppm; MS (ESI): m/z 289.7 $[M+H]^+$; Anal. calcd for $\text{C}_{15}\text{H}_{13}\text{ClN}_2\text{O}_2$: C 62.40, H 4.54, N 9.70, found: C 62.36, H 4.75, N 9.63.

Biology

Bacterial suppressive assay: The antibacterial activity of the synthesized compounds was tested against *E. coli* ATCC 25922, *P. aeruginosa* ATCC 27853, *S. aureus* ATCC 6538 and *B. subtilis* ATCC 530 (kindly provided by pro Chang-Hong Liu, State Key Laboratory of Pharmaceutical Biotechnology, Nanjing University, Nanjing) using Mueller-Hinton medium (MH medium: 17.5 g casein hydrolysate, 1.5 g soluble starch, 1000 mL beef extract). The minimum inhibitory concentration (MIC) values of the tested compounds were determined by a colorimetric method using 3-(4,5-dimethylthiazol-2-yl)-2,5-diphenyltetrazolium bromide (MTT). A stock solution of the test compound ($100 \mu\text{g mL}^{-1}$) in dimethyl sulfoxide (DMSO) was prepared, and graded quantities were added to a specified volume of sterilized liquid MH medium. A specified volume of the compound-containing medium was then poured into microtiter plates. A suspension of the microorganism was prepared to contain approx. 105 cfu mL^{-1} and applied to microtiter plates with serially

diluted compounds in DMSO to be tested and incubated at 37 °C for 24 h. After the MIC values were visually determined on each of the microtiter plates, phosphate buffered saline (PBS; 50 μ L, 0.01 M, pH 7.4; 2.9 g $\text{Na}_2\text{HPO}_4 \cdot 12\text{H}_2\text{O}$, 0.2 g KH_2PO_4 , 8.0 g NaCl, 0.2 g KCl, 1000 mL distilled H_2O) containing MTT (2 mg mL⁻¹) was added to each well. Incubation was continued at RT for 4–5 h. The content of each well was removed, and 100 μ L of isopropanol containing 5% HCl (final concentration 1 M) was added to extract the dye. After 12 h of incubation at RT, the optical density (OD) was measured with a microplate reader at 550 nm.

E. coli FabH inhibitory assay: Native *E. coli* FabH protein was overexpressed in *E. coli* DH10B cells using the pET30 vector (pET30 vector was kindly supplied by the State Key Laboratory of Pharmaceutical Biotechnology, Nanjing University) and purified to homogeneity in three chromatographic steps (Q-Sepharose, MonoQ, and hydroxyapatite) at 4 °C. The selenomethionine-substituted protein was expressed in *E. coli* BL21(DE3) cells and purified in a similar way. Harvested cells containing FabH were lysed by sonication in 20 mM Tris (pH 7.6) containing 5 mM imidazole and 0.5 M NaCl, and centrifuged (20000 rpm, 30 min, 4 °C). The supernatant was applied to a Ni-NTA agarose column, washed, and eluted using a 5–500 mM imidazole gradient over 20 column volumes. Eluted protein was dialyzed against 20 mM Tris (pH 7.6) containing 1 mM dithiothreitol (DTT) and 100 mM NaCl. Purified FabHs were concentrated to 2 mg mL⁻¹ and stored at –80 °C in 20 mM Tris (pH 7.6) containing 100 mM NaCl, 1 mM DTT, and 20% glycerol for enzymatic assay.

In a final 20 μ L reaction, 20 mM Na_2HPO_4 (pH 7.0) containing 0.5 mM DTT, 0.25 mM MgCl_2 , and 2.5 μ M holo-ACP were mixed with 1 nM FabH, and H_2O was added to 15 μ L. After 1 min incubation, a 2 μ L mixture of 25 μ M acetyl-CoA, 0.5 mM NADH, and 0.5 mM NADPH was added for FabH reaction for 25 min. The reaction was stopped by adding 20 μ L of ice-cold 50% trichloroacetic acid (TCA), incubating for 5 min on ice, and centrifuging to pellet the protein. The pellet was washed with 10% ice-cold TCA and re-suspended in 0.5 M NaOH (5 μ L). The incorporation of the ³H signal in the final product was read by liquid scintillation. When determining the IC₅₀ values, inhibitors were added from a concentrated DMSO stock such that the final concentration of DMSO did not exceed 2%.

Docking study

Molecular docking of compound **10** into the three-dimensional X-ray structure of *E. coli* FabH (PDB: 1HNJ)^[22] was carried out using Discovery Studio (v3.1) as implemented through the graphical user interface DS-CDOCKER protocol.^[20]

The 3D structures of the aforementioned compounds were constructed using Chem3D ultra 12.0 (Chemical Structure Drawing Standard; Cambridge Soft corporation, USA) and energy minimized by using MMFF94 with 5000 iterations and minimum RMS gradient of 0.10. The crystal structures of *E. coli* FabH (PDB: 1HNJ)^[22] complex were retrieved from the RCSB Protein Data Bank (<http://www.rcsb.org/pdb/>). All bound waters and ligands were eliminated from the protein and the polar hydrogen was added to the proteins.

Acknowledgements

This work was financed by the National Natural Science Foundation of China (grant no. J1103512).

Keywords: antibacterial agents · dioxygenated rings · FabH · inhibitors · β -ketoacyl-ACP synthase III

- [1] R. A. Daines, I. Pendrak, K. Sham, G. S. Van Aller, A. K. Konstantinidis, J. T. Lonsdale, C. A. Janson, X. Qiu, M. Brandt, S. S. Khandekar, C. Silverman, M. S. Head, *J. Med. Chem.* **2003**, *46*, 5–8.
- [2] Z. Nie, C. Perretta, J. Lu, Y. Su, S. Margosiak, K. S. Gajiwala, J. Cortez, V. Nikulin, K. M. Yager, K. Appelt, S. Chu, *J. Med. Chem.* **2005**, *48*, 1596–1609.
- [3] K. S. Gajiwala, S. Margosiak, J. Lu, J. Cortez, Y. Su, Z. Nie, K. Appelt, *FEBS Lett.* **2009**, *583*, 2939–2946.
- [4] M. M. Alhamadsheh, N. C. Waters, S. Sachdeva, P. Lee, K. A. Reynolds, *Bioorg. Med. Chem. Lett.* **2008**, *18*, 6402–6405.
- [5] J. Lee, K. Jeong, S. Shin, J. Lee, Y. Kim, *Eur. J. Med. Chem.* **2012**, *47*, 261–269.
- [6] A. Ashek, S. J. Cho, *Bioorg. Med. Chem.* **2006**, *14*, 1474–1482.
- [7] S. Singh, L. K. Soni, M. K. Gupta, Y. S. Prabhakar, S. G. Kaskhedikar, *Eur. J. Med. Chem.* **2008**, *43*, 1071–1080.
- [8] S. Brinster, G. Lamberet, B. Staels, P. Trieu-Cuot, A. Gruss, C. Poyart, *Nature* **2009**, *458*, 83–86.
- [9] W. Balemans, N. Lounis, R. Gilissen, J. Guillemont, K. Simmen, K. Andries, A. Koul, *Nature* **2010**, *463*, E3.
- [10] J. B. Parsons, C. O. Rock, *Curr. Opin. Microbiol.* **2011**, *14*, 544–549.
- [11] D. Payne, W. Miller, V. Berry, J. Brosky, W. Burgess, E. Chen, W. DeWolf, Jr., A. Fosberry, R. Greenwood, M. Head, D. Heering, C. Janson, D. Jaworski, P. Keller, P. Manley, T. Moore, K. Newlander, S. Pearson, B. Polizzi, X. Qiu, S. Rittenhouse, C. Slater-Radosti, K. Salyers, M. Seefeld, M. Smyth, D. Takata, I. Uzinskas, K. Vaidya, N. Wallis, S. Winram, C. Yuan, W. Huffman, *Antimicrob. Agents Chemother.* **2002**, *46*, 3118–3124.
- [12] W. H. Miller, M. A. Seefeld, K. A. Newlander, I. N. Uzinskas, W. J. Burgess, D. A. Heering, C. C. K. Yuan, M. S. Head, D. J. Payne, S. F. Rittenhouse, T. D. Moore, S. C. Pearson, V. Berry, W. E. DeWolf, P. M. Keller, B. J. Polizzi, X. Qiu, C. A. Janson, W. F. Huffman, *J. Med. Chem.* **2002**, *45*, 3246–3256.
- [13] J. R. Miller et al., *Proc. Natl. Acad. Sci. USA* **2009**, *106*, 1737–1742.
- [14] C. McInnes, *Curr. Opin. Chem. Biol.* **2007**, *11*, 494–502.
- [15] J. Kirchmair, S. Ristic, K. Eder, P. Markt, G. Wolber, C. Laggner, T. Langer, *J. Chem. Inf. Model.* **2007**, *47*, 2182–2196.
- [16] P. D. Kirchhoff, R. Brown, S. Kahn, M. Waldman, C. M. Venkatachalam, *J. Comput. Chem.* **2001**, *22*, 993–1003.
- [17] S. D. Pickett, J. S. Mason, I. M. McLay, *J. Chem. Inf. Comput. Sci.* **1996**, *36*, 1214–1223.
- [18] M. Elhallaoui, M. Laguerre, A. Carpy, F. C. Ouazzani, *J. Mol. Model.* **2002**, *8*, 65–72.
- [19] J. Lee, K. Jeong, J. Lee, D. Kang, Y. Kim, *Bioorg. Med. Chem.* **2009**, *17*, 1506–1513.
- [20] Discovery Studio 3.1, Accelrys Software Inc., San Diego, CA (USA), **2011**.
- [21] D. D. Li, F. Fang, J. R. Li, Q. R. Du, J. Sun, H. B. Gong, H. L. Zhu, *Bioorg. Med. Chem. Lett.* **2012**, *22*, 5870–5875.
- [22] X. Qiu, C. A. Janson, W. W. Smith, M. Head, J. Lonsdale, A. K. Konstantinidis, *J. Mol. Biol.* **2001**, *307*, 341–356.

Received: December 25, 2012

Published online on February 7, 2013